Supplementary Information

Supplementary FIGURES

Figure S1

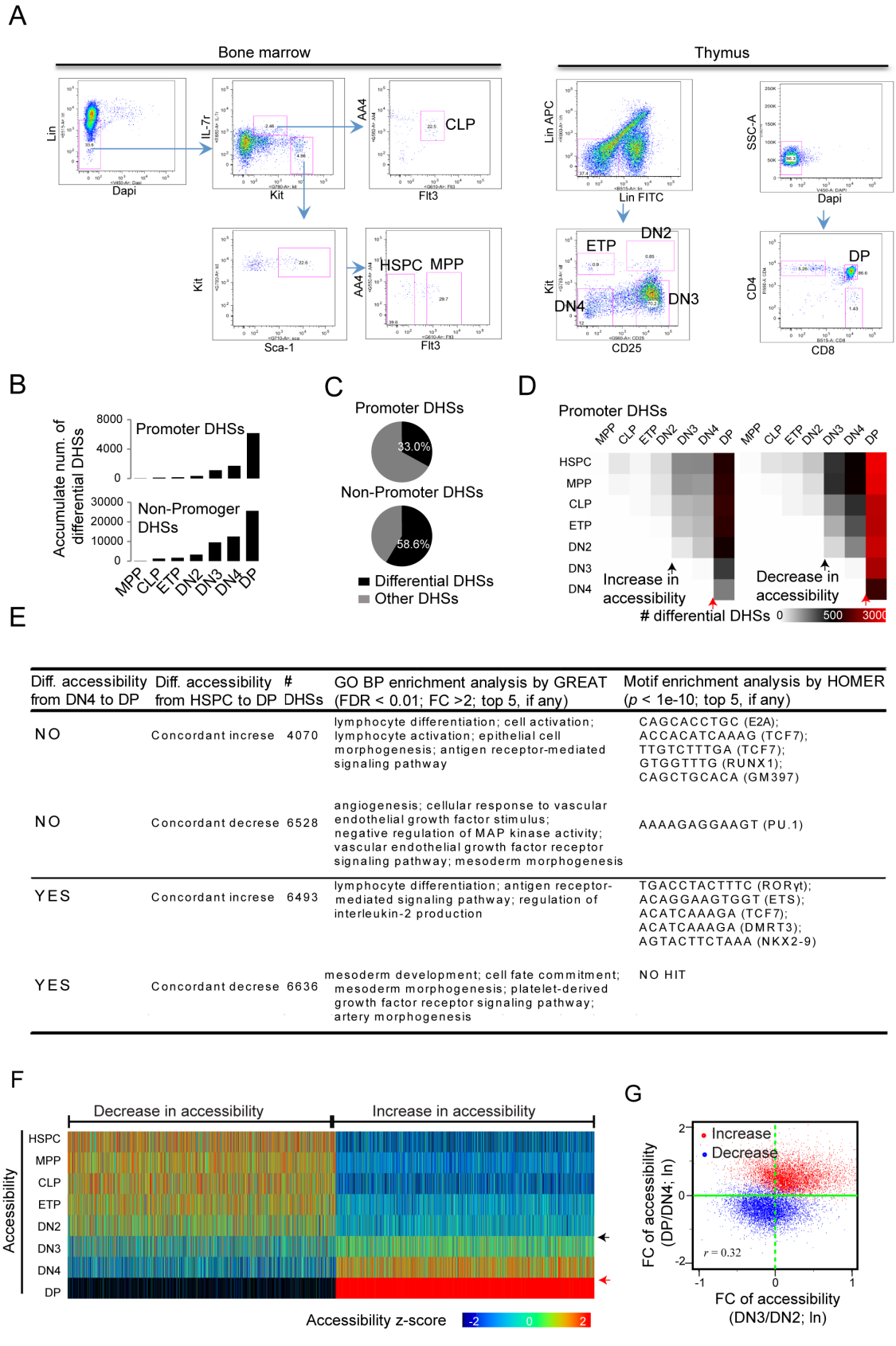

E

Diff. accessibility from DN4 to DP	Diff. accessibility from HSPC to DP	# DHSs	GO BP enrichment analysis by GREAT (FDR < 0.01; FC >2; top 5, if any)	Motif enrichment analysis by HOMER (p < 1e-10; top 5, if any)
NO	Concordant increse	4070	lymphocyte differentiation; cell activation; lymphocyte activation; epithelial cell morphogenesis; antigen receptor-mediated signaling pathway	CAGCACCTGC (E2A); ACCACATCAAAG (TCF7); TTGTCTTTGA (TCF7); GTGGTTTG (RUNX1); CAGCTGCACA (GM397)
NO	Concordant decrese	6528	angiogenesis; cellular response to vascular endothelial growth factor stimulus; negative regulation of MAP kinase activity; vascular endothelial growth factor receptor signaling pathway; mesoderm morphogenesis	AAAAGAGGAAGT (PU.1)
YES	Concordant increse	6493	lymphocyte differentiation; antigen receptor-mediated signaling pathway; regulation of interleukin-2 production	TGACCTACTTTC (RORγt); ACAGGAAGTGGT (ETS); ACATCAAAGA (TCF7); ACATCAAAGA (DMRT3); AGTACTTCTAAA (NKX2-9)
YES	Concordant decrese	6636	mesoderm development; cell fate commitment; mesoderm morphogenesis; platelet-derived growth factor receptor signaling pathway; artery morphogenesis	NO HIT

Figure S1: Change of chromatin accessibility at the DN4-to-DP transition follows that at the DN2-to-DN3 transition – **related to Figure 1**

(A) FACS profiles for isolating HSPC, MPP and CLP cells from bone marrow and for isolating ETP, DN2, DN3, DN4, and DP cells from thymus.

(B) Accumulative number of differential DHSs in promoter regions (upper panel) and non-promoter regions (lower panel) from HSPC to flowing stages from MPP to DP cells.

(C) Pie graph showing the distribution of differential DHSs in promoter regions (upper panel) and non-promoter regions (lower panel).

(D) Heat map showing the numbers of differential DHSs in promoter regions, increasing (left panel) or decreasing (right panel) in chromatin accessibility, for any two stages from HSPC to DP. Black and red arrow heads: DN2-to-DN3 transition and the DN4-to-DP transition, respectively.

(E) GREAT Gene Ontology enrichment analysis and HOMER motif enrichment analysis for DHSs with concordant change in accessibility from HSPC to DP, sorted first based on the change in accessibility at the DN4-to-DP transition and then by the direction of concordant change in accessibility across all stages from HSPC to DP cells.

(F) Heat map visualization of scDNase-Seq read density for non-promoter DHSs that show differential accessibility between DN4 and DP cells, sorted based on concordant increase or decrease in chromatin accessibility from HSPC to DP cells. Black and red arrowheads: the DN2-to-DN3 transition and the DN4-to-DP transition, respectively.

(G) Scatter plot for the change in the z-score of scDNase-Seq read density at DN2-to-DN3 transition and at the DN4-to-DP transition for the same group of DHSs from panel **F**. *r*: Pearson's correlation coefficient.

Figure S2

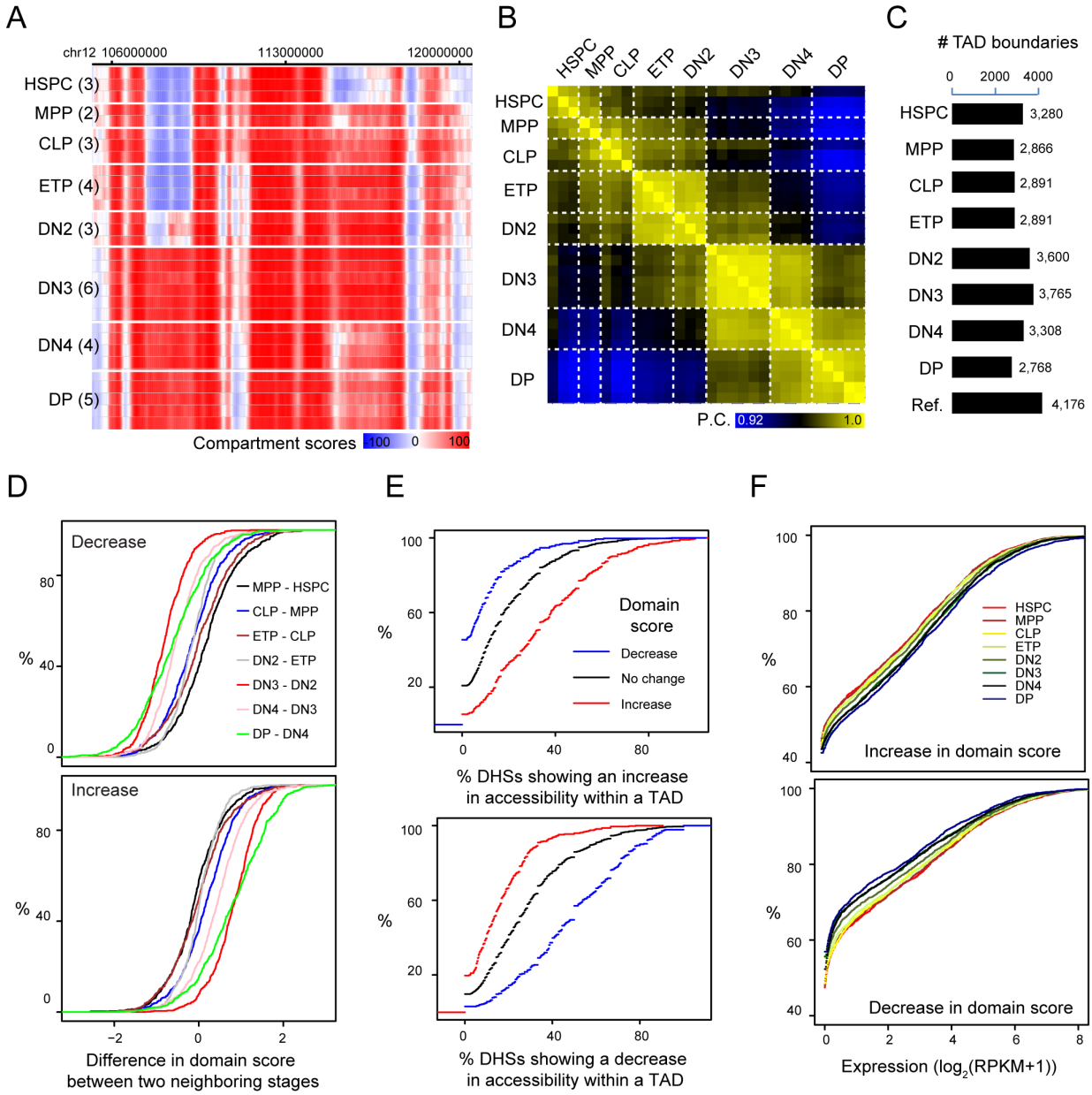
A
chr12 106000000
113000000
120000000
HSPC (3)
MPP (2)
CLP (3)
ETP (4)
DN2 (3)
DN3 (6)
DN4 (4)
DP (5)
Compartment scores -100 0 100
B
HSPC
MPP
CLP
ETP
DN2
DN3
DN4
DP
P.C. 0.92 1.0
C
TAD boundaries
0 2000 4000
HSPC 3,280
MPP 2,866
CLP 2,891
ETP 2,891
DN2 3,600
DN3 3,765
DN4 3,308
DP 2,768
Ref. 4,176
D
Decrease
MPP - HSPC
CLP - MPP
ETP - CLP
DN2 - ETP
DN3 - DN2
DN4 - DN3
DP - DN4
Increase
%
Difference in domain score
between two neighboring stages
E
Domain score
Decrease
No change
Increase
% DHSs showing an increase
in accessibility within a TAD
% DHSs showing a decrease
in accessibility within a TAD
F
HSPC
MPP
CLP
ETP
DN2
DN3
DN4
DP
Increase in domain score
Decrease in domain score
Expression (log2(RPKM+1))

Figure S2: Coordinated change of intra-TAD connectivity and chromatin accessibility at enclosing DHSs – **related to Figure 2**

(A) Heat map showing the distribution of compartment score across a 14M bps genomic region in chromosome 12 for all replicates of Hi-C libraries prepared for each developmental stage from HSPC to DP. Number in parentheses: number of replicates for each stage.

(B) Heat map showing the Pearson's correlation coefficients of compartment scores across all 20K bps genomic bins for a pair-wise comparison of all Hi-C libraries.

(C) Numbers of TAD boundaries identified for each developmental stage and number of TAD boundaries pooled from all stages, termed as the reference boundaries.

(D) Empirical cumulative distributions of the difference in z-score of domain scores between every two consecutive stages for TAD showing a decrease (upper panel) or increase (lower panel) in domain scores. Y-axis records the % of TAD with a difference in domain score lower than the one when specified by the X-axis.

(E) Empirical cumulative distribution of the % of DHSs that show increase (top panel) or decrease (bottom panel) in accessibility within TADs for TADs sorted based on the change of domain score from HSPC to DP.

(F) Empirical cumulative distribution of expression values for genes extracted from TADs with an increase (upper panel) or decrease (lower panel) in domain scores.

Figure S3

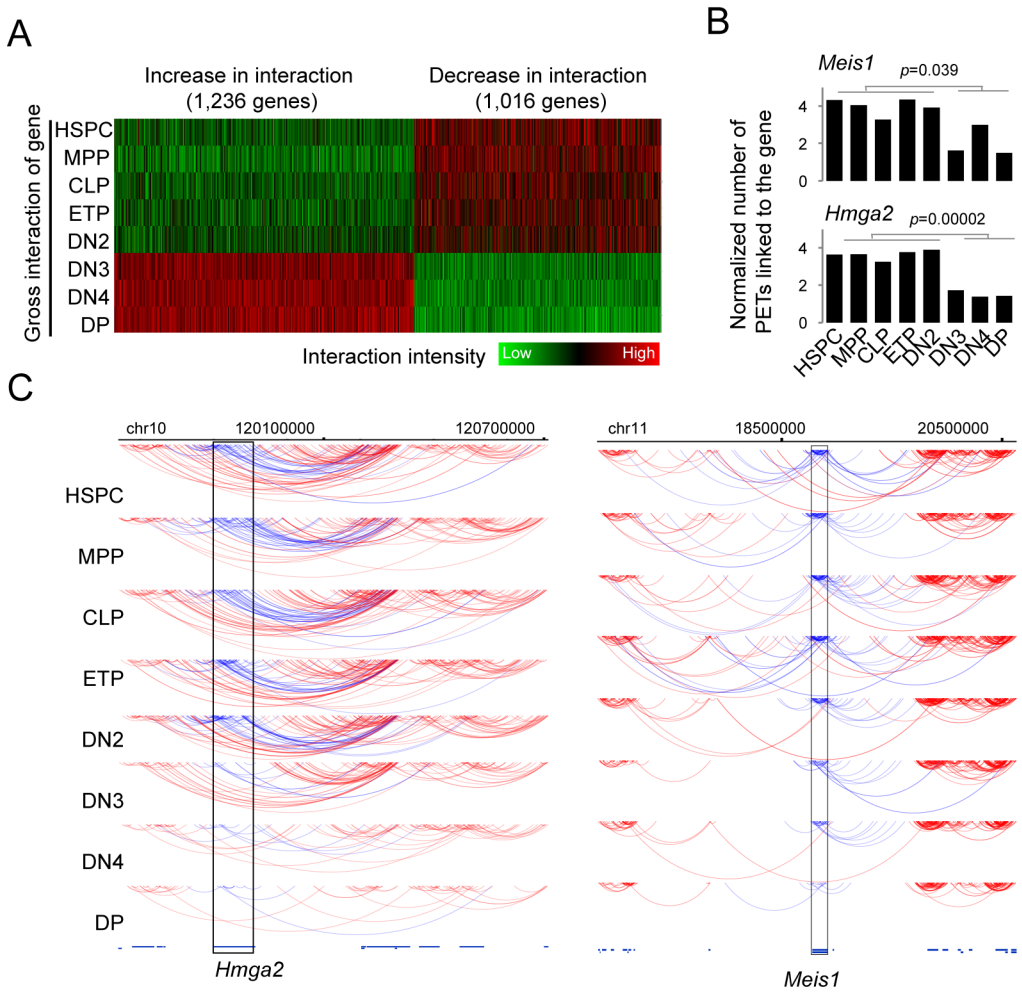

Figure S3: Genes with a substantial decrease in interaction are gradually silenced – **related to Figure 3**

(A) Heat map of interaction density from HSPC to the DP stage for genes that showed significant increase or decrease in the number of gross interaction before and after T cell commitment.

(B) Bar graphs showing examples of genes with a substantial decrease (*Hmga2* and *Meis1*) in the number of gross interacting PETs linked to the genes before and after T cell commitment. *P*-value by *t*-test.

(C) Arc plot from WashU epigenome browser showing the gross interacting PETs of *Hmga2* (left panel) and *Meis1* (right panel) from HSPC to DP cells. Blue lines: PETs with at least one end linking to *Hmga2* (or *Meis1*) locus (indicated by rectangles). Pooled from 2-5 independent experiments.

Figure S4

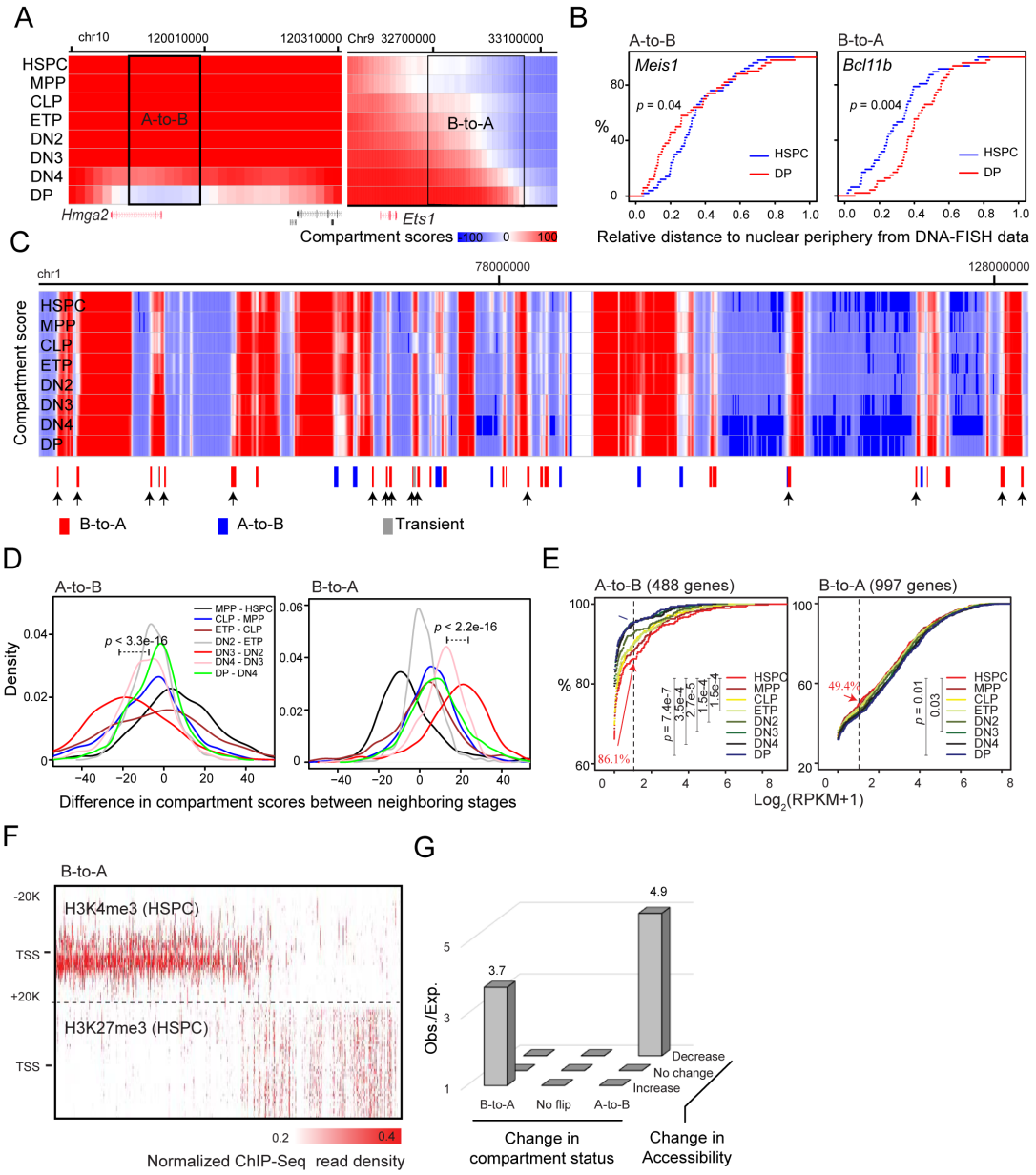
A
chr10
120010000
120310000
Chr9
32700000
33100000
HSPC
MPP
CLP
ETP
DN2
DN3
DN4
DP
A-to-B
B-to-A
Hmga2
Ets1
Compartment scores
100
0
100
B
A-to-B
B-to-A
Meis1
Bcl11b
p = 0.04
p = 0.004
%
HSPC
DP
Relative distance to nuclear periphery from DNA-FISH data
C
chr1
78000000
128000000
Compartment score
B-to-A
A-to-B
Transient
D
A-to-B
B-to-A
Density
p < 3.3e-16
p < 2.2e-16
MPP - HSPC
CLP - MPP
ETP - CLP
DN2 - ETP
DN3 - DN2
DN4 - DN3
DP - DN4
Difference in compartment scores between neighboring stages
E
A-to-B (488 genes)
B-to-A (997 genes)
86.1%
49.4%
Log2(RPKM+1)
F
B-to-A
-20K
TSS
+20K
TSS
H3K4me3 (HSPC)
H3K27me3 (HSPC)
Normalized ChIP-Seq read density
G
Obs./Exp.
4.9
3.7
Decrease
No change
Increase
B-to-A
No flip
A-to-B
Change in compartment status
Change in Accessibility

Figure S4: Correlation of compartment reorganization and change in expression and chromatin states – **related to Figure 4**

(A) Heat maps showing the distributions of compartment score across genomic regions encompassing *Hmga2* (left panel) and *Ets1* (right panel), for each developmental stage from HSPC to DP. Rectangles: genomic regions with a compartment flip. Pooled from 2-5 independent experiments (also applied to C).

(B) Empirical cumulative distribution of the relative distance to nuclear periphery for *Meis1* locus (left panel) and *Bcl11b* locus (right panel) in HSPC cells (blue line; 28 cells) and in DP cells (red line; 30 cells), with a line shifting to the left side indicating a closer distance to the periphery. *P*-value by Kolmogorov-Smirnov test.

(C) Heat maps showing the distributions of compartment score across a 100M genomic region in chromosome 1, with flipped compartment regions indicated. Arrow heads: regions with B-to-A flip occurring at compartment boundaries.

(D) Distribution of the difference in compartment scores between every two neighboring stages for genomic regions showing concordant A-to-B compartment flips (left panel) and concordant B-to-A compartment flips (right panel). *P*-value by Kolmogorov-Smirnov test.

(E) Empirical cumulative distribution of expression values for genes extracted from A-to-B flipped compartments (left panel) or from B-to-A flipped compartments (right panel) for each developmental stage. Y-axis: the percentage of genes with expression values lower than the one when specified by the X-axis. A line shifting to the left side corresponds to a generally lower expression within the population. Dotted vertical line: an RPKM value of 1, a cutoff to separate expressed and non-expressed genes. *P*-value by Kolmogorov-Smirnov test.

(F) Distribution of active histone modification H3K4me3 and repressive histone modification H3K27me3 in HSPC cells surrounding TSS (±20K bps) of genes extracted from B-to-A flipped compartments.

(G) 3D bar graphs for the ratios of observed (Obs.) to expected (Exp.) number for DHSs grouped based on their change in chromatin accessibility at the DN2-to-DN3 transition and their change in compartment status during early T cell development.

Figure S5

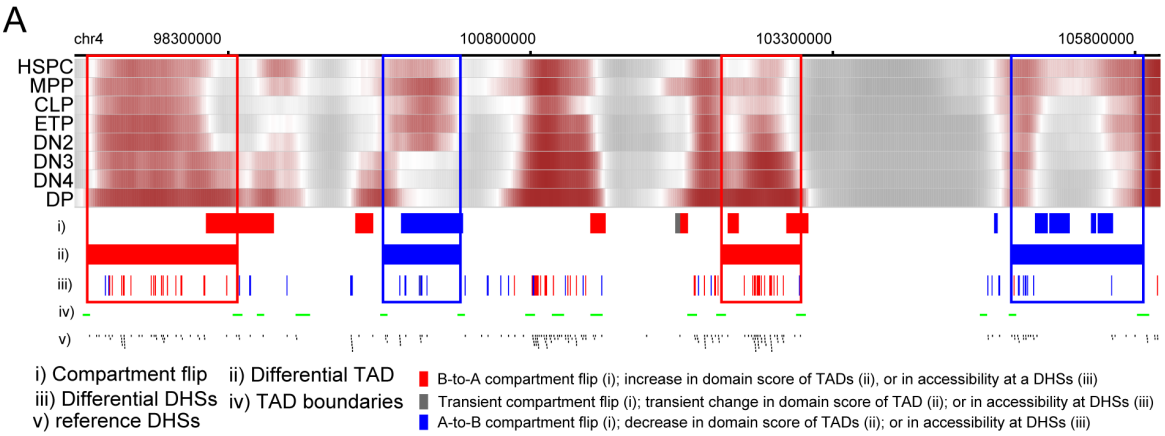
A
chr4
98300000
100800000
103300000
105800000
HSPC
MPP
CLP
ETP
DN2
DN3
DN4
DP
i)
ii)
iii)
iv)
v)
i) Compartment flip
ii) Differential TAD
iii) Differential DHSs
iv) TAD boundaries
v) reference DHSs
B-to-A compartment flip (i); increase in domain score of TADs (ii), or in accessibility at a DHSs (iii)
Transient compartment flip (i); transient change in domain score of TAD (ii); or in accessibility at DHSs (iii)
A-to-B compartment flip (i); decrease in domain score of TADs (ii); or in accessibility at DHSs (iii)

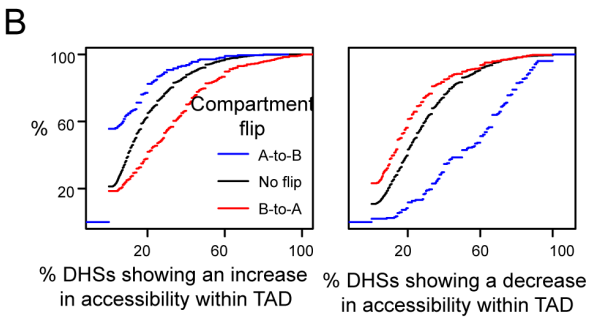
B
100
%
60
20
Compartment flip
A-to-B
No flip
B-to-A
20
60
100
% DHSs showing an increase in accessibility within TAD
% DHSs showing a decrease in accessibility within TAD

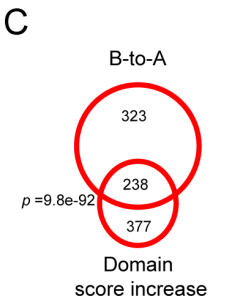
C
B-to-A
323
238
377
p =9.8e-92
Domain score increase

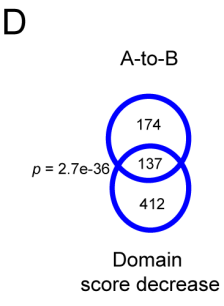
D
A-to-B
174
137
412
p = 2.7e-36
Domain score decrease

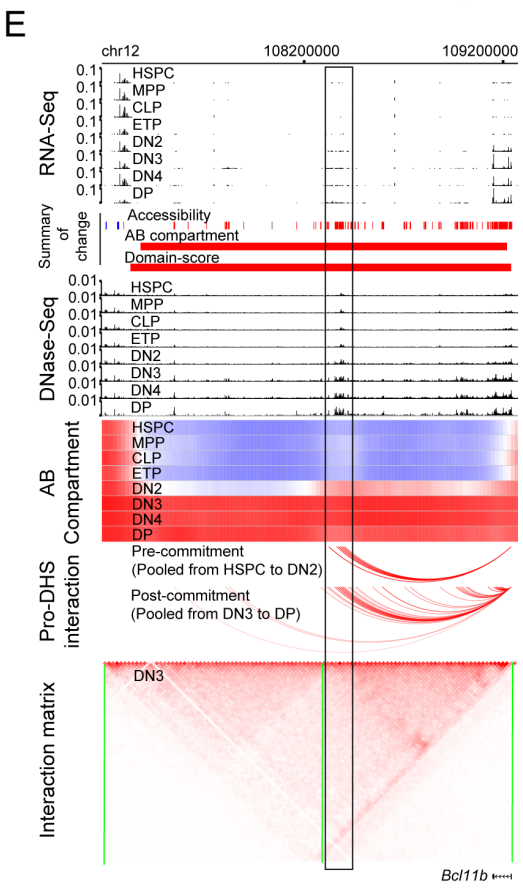
E
chr12
108200000
109200000
RNA-Seq
HSPC
MPP
CLP
ETP
DN2
DN3
DN4
DP
Summary of change
Accessibility
AB compartment
Domain-score
DNase-Seq
AB Compartment
Pro-DHS interaction
Pre-commitment
(Pooled from HSPC to DN2)
Post-commitment
(Pooled from DN3 to DP)
Interaction matrix
Bcl11b

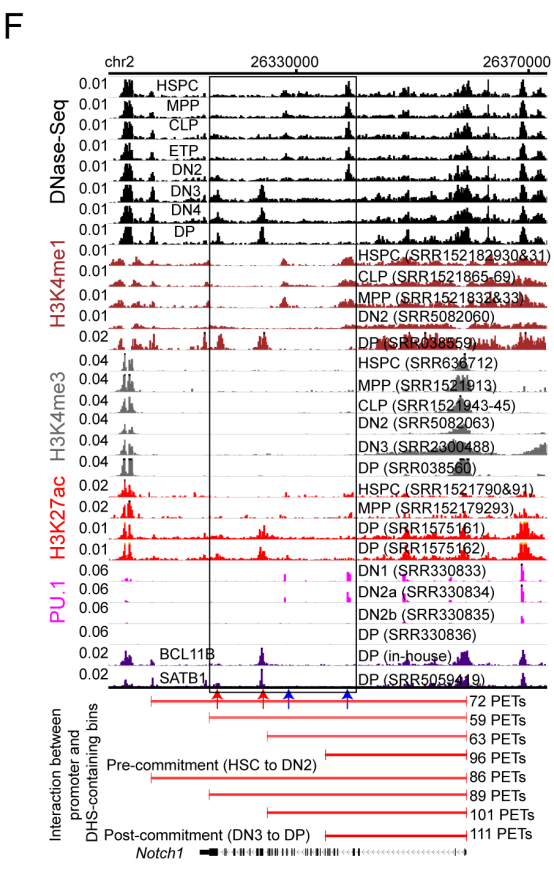
F
chr2
26330000
26370000
DNase-Seq
H3K4me1
H3K4me3
H3K27ac
PU.1
HSPC (SRR1521829&30&31)
CLP (SRR1521865-69)
MPP (SRR1521832&33)
DN2 (SRR5082060)
DP (SRR038559)
HSPC (SRR636712)
MPP (SRR1521913)
CLP (SRR1521943-45)
DN2 (SRR5082063)
DN3 (SRR2300488)
DP (SRR038560)
HSPC (SRR1521790&91)
MPP (SRR1521792&93)
DP (SRR1575161)
DP (SRR1575162)
DN1 (SRR330833)
DN2a (SRR330834)
DN2b (SRR330835)
DP (SRR330836)
BCL11B
SATB1
DP (in-house)
DP (SRR5059419)
Interaction between promoter and DHS-containing bins
72 PETs
59 PETs
63 PETs
96 PETs
Pre-commitment (HSC to DN2)
86 PETs
89 PETs
101 PETs
Post-commitment (DN3 to DP)
111 PETs
Notch1

Figure S5: Coordinated change of A/B compartments, TAD connectivity and DHS accessibility – **related to Figure 5**

(A) An integrative view of compartment flips (panel i), change in intra-TAD connectivity (panel ii), and change in chromatin accessibility at DHSs (panel iii) for a ~9.5M genomic region in chromosome 4. Top panel: heat maps for the distribution of compartment scores for each stage, pooled from 2-5 independent experiments; panel iv) positions of the reference TAD boundaries; v) positions of the reference DHSs. Red rectangles: TADs that overlap with B-to-A flipped compartments, show an increase in domain score, and harbor DHSs showing a general increase in accessibility. Blue rectangles: TADs that overlap with A-to-B flipped compartments, show a decrease in domain score, and harbor DHSs showing an overall decrease in accessibility.

(B) Empirical cumulative distribution of the % of DHSs that show increase (left panel) or decrease (right panel) in accessibility within TADs. Three groups of TADs are compared: those overlapping with B-to-A flipped compartments, those overlapping with A-to-B compartments and those showing no compartment flip.

(C) Venn diagram for the numbers of TADs that show both an overlap with B-to-A flipped compartment and an increase in domain scores (the shared part), or show only an overlap with B-to-A flipped compartment (top part) or show only an increase in domain score (bottom part). *P*-value by binomial test.

(D) Venn diagram for the numbers of TADs that show both an overlap with A-to-B flipped compartment and a decrease in domain scores (the shared part), or show only an overlap with A-to-B flipped compartment (top part) or show only a decrease in domain score (bottom part). *P*-value by binomial test.

(E) Online WashU genome browser session showing tracks for RNA-Seq reads (n=2), DNase-Seq reads (n=2), and A/B compartment score (pooled from n = 2-5) for a genomic region surrounding a super-enhancer of *Bcl11b* (rectangle) from HSPCs to DPs. Summary of change: tracks that summarizes change in accessibility at DHSs, A/B compartmental status, and domain score within TADs with color encoded the same as that of panel i-iii in **A**. Green lines: TAD boundaries; arc plots: Fit-HiC predicted interaction between *Bcl11b* promoter and DHS-containing genomic bins (q-value < 0.01). The predictions were made at a resolution of 10K bp for stages pooled from HSC to DN2 (pre-commitment) and for stages pooled from DN3 to DP (post-commitment) to increase statistic power (also applied to panel **F**). Interaction matrix: shown only for DN2 to save space. n: number of independent experiments;

(F) Online WashU genome browser session showing tracks for DNase-Seq data (number of independent experiments = 2), representative ChIP-Seq data of H3K4me1, H3K4me2, H3K4me3, H3K27ac, PU.1, BCL11B and SATB1 for stages where data is available, and Fit-HiC predicted interaction (q-value < 0.01) between DHS-containing bins and *Notch1* promoter at a resolution of 10Kbp for stages pre-commitment (pooled from HSC to DN2) and post-commitment (pooled from DN3 to DP). Red arrow heads: DHSs increasing in

accessibility; Blue arrow heads: DHSs decreasing in accessibility; Black rectangle: region of enhancer switch; parenthesis: accession number for public data.

Figure S6

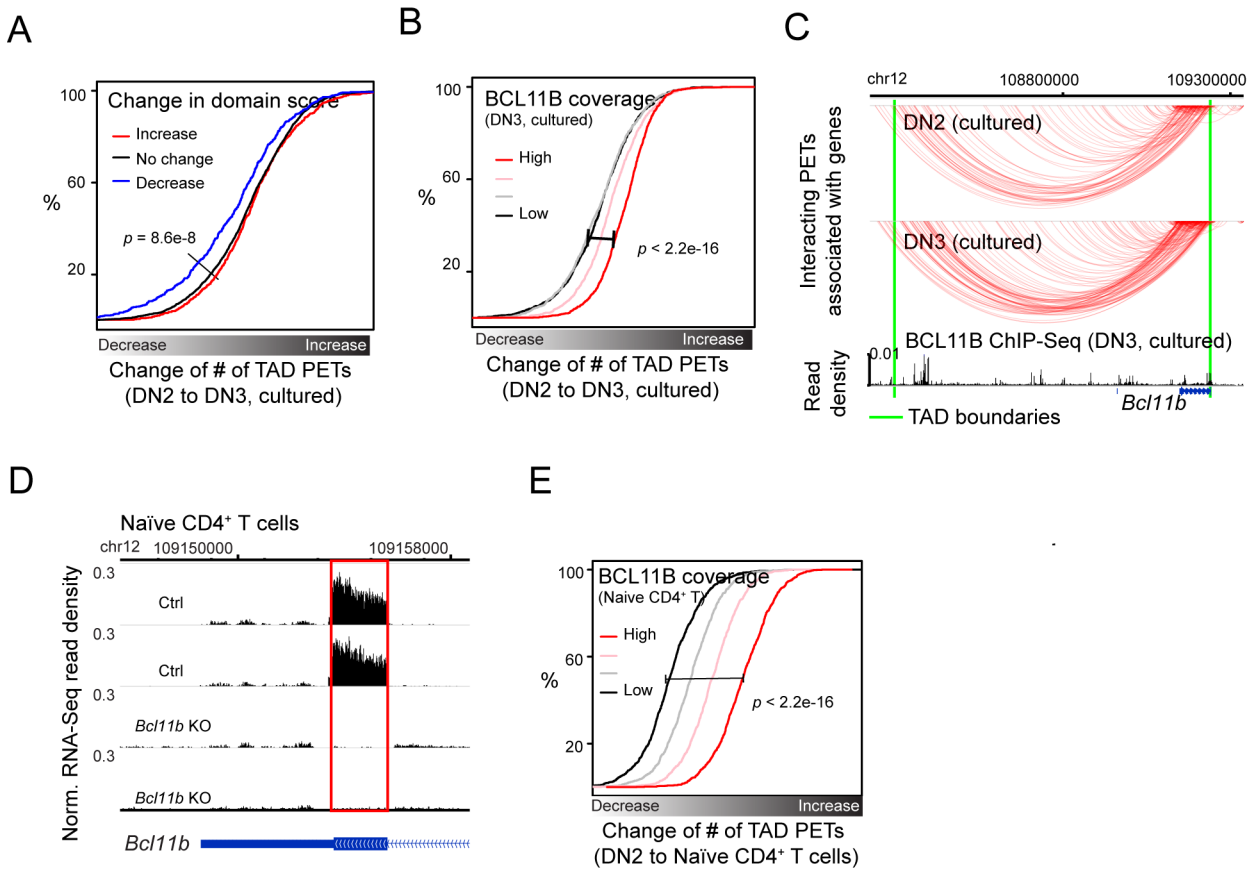

Figure S6: Increase of intra-TAD connectivity is associated with BCL11B binding – **related to Figures 6&7**

(A) Empirical cumulative distribution of the fold change of the number of all TAD PETs from DN2 to DN3 cells, both bone marrow-derived cultured for TADs sorted based on their change in intra-TAD connectivity (or domain score) during early T cells development from HSCs to DPs (primary cells). *P*-value by Kolmogorov-Smirnov test (also applied to panels B and E.

(B) Empirical cumulative distribution of the fold change of the number of all TAD PETs from DN2 to DN3 cells, both bone marrow-derived cultured for TADs sorted into four equal size groups based on the their BCL11B coverages in the cultured DN3 cells.

(C) WashU genome browser showing the distribution of TAD PETs in BM-derived DN2 and DN3 cells (one independent experiment) and the distribution of BCL11B ChIP-Seq reads in BM-derived DN3 for a TAD enclosing *Bcl11b*. Green lines: TAD boundaries.

(D) WashU genome browser image showing the RNA-Seq read distribution surrounding the last exon of *Bcl11b*, targeted for deletion (highlighted red in rectangle), in control and *Bcl11b* deleted Naïve CD4+ T cells.

(E) Empirical cumulative distribution of the fold change of the number of TAD PETs from DN2 to Naïve $CD4^+$ T cells for TADs sorted into four equal size groups based on their BCL11B coverages in DPs.